Electron Transfer in Ruthenium/Zinc Porphyrin Derivatives of Recombinant Human Myoglobins. Analysis of Tunneling Pathways in Myoglobin and Cytochrome c

Danilo R. Casimiro, Luet-L. Wong,[1a] Jorge L. Colón,[1b] Thomas E. Zewert, John H. Richards, I-Jy Chang, Jay R. Winkler,* and Harry B. Gray*

Contribution No. 8716 from the Beckman Institute, California Institute of Technology, Pasadena, California 91125. Received August 28, 1992

Abstract: Site-directed mutants of human myoglobin have been prepared and characterized; each protein has a single surface-modifiable histidine (at position 48, 70, or 83). The proteins were modified by covalent attachment of pentaammineruthenium (a_5Ru) to the surface histidine and substitution of zinc mesoporphyrin IX diacid (ZnP) for the heme. Donor-acceptor separations (edge-edge distances d) in the modified proteins are 9.5 Å, His70; 12.7 Å, His48; and 15.5 Å, His83. Rates of photoinduced electron transfer in these ruthenium-modified myoglobins were measured by transient absorption spectroscopy. The $^3ZnP^* \rightarrow Ru^{3+}$ rate constants are 1.6×10^7 (His70), 7.2×10^4 (His48), and 4.0×10^2 s^{-1} (His83) ($-\Delta G^\circ = 0.82$ eV); charge-recombination ($Ru^{2+} \rightarrow ZnP^+$) rates are 1.1×10^5 (His48) and 7.3×10^2 s^{-1} (His83) ($-\Delta G^\circ = 0.96$ eV). Activationless (maximum) rates assuming $\lambda = 1.3$ eV are 7.2×10^7 (His70), 3.3×10^5 (His48), and 1.8×10^3 s^{-1} (His83). Distant electronic couplings, which limit the maximum rates in the modified myoglobins, have been analyzed along with data from Ru-modified cytochromes c in terms of a tunneling pathway model. Single dominant pathways adequately describe the electronic couplings in cytochrome c but do not satisfactorily account for the myoglobin couplings. The correlation of electronic coupling with tunneling length for myoglobin is improved significantly by the inclusion of multiple pathways.

Introduction

Both theoretical and experimental investigations have shown that variations in distant donor-acceptor (D-A) electronic couplings can control the rates of many protein electron-transfer (ET) reactions.[2-19] If a simple homogeneous medium separates donor and acceptor, then the coupling is expected to decay exponentially with increasing D-A distance d (eq 1).[2] In this expression, H_{AB}°

$$H_{AB} = H_{AB}^\circ \exp[-\beta(d - d_0)/2] \quad (1)$$

is the matrix element at van der Waals contact ($d_0 \sim 3$ Å) and β is the distance decay factor. Commonly observed β values in covalently coupled D-A systems and randomly oriented D-A systems in rigid matrices are between 0.8 and 1.2 $Å^{-1}$.[20-26] The main difference between these systems and proteins is the distinct nature of the medium between redox sites. Synthetic D-A complexes tend to have rather direct, covalently linked pathways from donor to acceptor. The medium between redox sites in a protein, however, is a heterogeneous array of bonded and nonbonded interactions. Direct D-A coupling is extremely weak at the distances considered here (>10 Å); the intervening polypeptide must mediate the donor-acceptor interaction. Dutton and coworkers have recently examined activationless intramolecular ET rates in a variety of biological systems.[18] They find that these data are well-described by an exponential-decay-with-distance model: $\beta = 1.4$ $Å^{-1}$; k_{max} ($d = 3$ Å) $= 1 \times 10^{13}$ s^{-1}). This analysis, which compares ET rates from many different protein systems, supports the notion that the intervening polypeptide behaves as a homogeneous medium.

(1) (a) Present address: Inorganic Chemistry Laboratory, University of Oxford, South Parks Road, Oxford OX1 3QR, U.K. (b) Present address: Department of Chemistry, University of Puerto Rico, Río Piedras, Puerto Rico 00931.

(2) Marcus, R. A.; Sutin, N. *Biochim. Biophys. Acta* **1985**, *811*, 265.

(3) McLendon, G. *Acc. Chem. Res.* **1988**, *21*, 160.

(4) Bertrand, P. *Struct. Bonding* **1991**, *75*, 1.

(5) Kuki, A. *Struct. Bonding* **1991**, *75*, 49.

(6) Beratan, D. N.; Betts, J. N.; Onuchic, J. N. *Science* **1991**, *252*, 1285.

(7) (a) Beratan, D. N.; Onuchic, J. N.; Hopfield, J. J. *J. Chem. Phys.* **1987**, *86*, 4488. (b) Beratan, D. N.; Onuchic, J. N. *Photosynth. Res.* **1989**, *22*, 173. (c) Beratan, D. N.; Onuchic, J. N.; Betts, J. N.; Bowler, B. E.; Gray, H. B. *J. Am. Chem. Soc.* **1990**, *112*, 7915. (d) Onuchic, J. N.; Beratan, D. N. *J. Chem. Phys.* **1990**, *92*, 722. (e) Onuchic, J. N.; Andrade, P. C. P.; Beratan, D. N. *J. Chem. Phys.* **1991**, *95*, 1131. (f) Beratan, D. N.; Betts, J. N.; Onuchic, J. N. *J. Phys. Chem.* **1992**, *96*, 2852. (g) Betts, J. N.; Beratan, D. N.; Onuchic, J. N. *J. Am. Chem. Soc.* **1992**, *114*, 4043.

(8) (a) Siddarth, P.; Marcus, R. A. *J. Phys. Chem.* **1990**, *94*, 8430. (b) Siddarth, P.; Marcus, R. A. *J. Phys. Chem.* **1992**, *96*, 3213.

(9) (a) Kuki, A.; Wolynes, P. G. *Science* **1987**, *236*, 1647. (b) Gruschus, J. M.; Kuki, A., in preparation. (c) Gruschus, J. M.; Kuki, A. *Chem. Phys. Lett.* **1992**, *192*, 205.

(10) Broo, A.; Larsson, S. *J. Phys. Chem.* **1990**, *94*, 4925.

(11) (a) Christensen, H. E. M.; Conrad, L. S.; Mikkelsen, K. V.; Nielsen, M. K.; Ulstrup, J. *Inorg. Chem.* **1990**, *29*, 2808. (b) Christensen, H. E. M.; Conrad, L. S.; Mikkelsen, K. V.; Ulstrup, J. *J. Phys. Chem.* **1992**, *96*, 4451.

(12) Goldman, C. *Phys. Rev. A* **1991**, *43*, 4500.

(13) *Metal Ions in Biological Systems*; Sigel, H., Sigel, A., Eds.; Dekker: New York, 1991; Vol. 27.

(14) (a) Liang, N.; Pielak, G.; Mauk, A. G.; Smith, M.; Hoffman, B. M. *Proc. Natl. Acad. Sci. U.S.A.* **1987**, *84*, 1249. (b) Liang, N.; et al. *Science* **1988**, *240*, 311. (c) Everest, A. M.; Wallin, S. A.; Stemp, E. D. A.; Nocek, J. M.; Mauk, A. G.; Hoffman, B. M. *J. Am. Chem. Soc.* **1991**, *113*, 4337.

(15) Farver, O.; Pecht, I. *FEBS Lett.* **1989**, *244*, 376, 379.

(16) (a) Bowler, B. E.; Meade, T. J.; Mayo, S. L.; Richards, J. H.; Gray, H. B. *J. Am. Chem. Soc.* **1989**, *111*, 8757. (b) Cowan, J. A.; Upmacis, R. K.; Beratan, D. N.; Onuchic, J. N.; Gray, H. B. *Ann. N. Y. Acad. Sci.* **1989**, *550*, 68. (c) Therien, M. J.; Bowler, B. E.; Selman, M. A.; Gray, H. B.; Chang, I.-J.; Winkler, J. R. In *Electron Transfer in Inorganic, Organic, and Biological Systems*; Bolton, J. R., Mataga, N., McLendon, G., Eds.; Advances in Chemistry 228; American Chemical Society: Washington, DC, 1991; pp 191-199. (d) Jacobs, B. A.; Mauk, M. R.; Funk, W. D.; MacGillivray, R. T. A.; Mauk, A. G.; Gray, H. B. *J. Am. Chem. Soc.* **1991**, *113*, 4390. (e) Therien, M. J.; Chang, J.; Raphael, A. L.; Bowler, B. E.; Gray, H. B. *Struct. Bonding* **1991**, *75*, 109. (f) Wuttke, D. S.; Bjerrum, M. J.; Winkler, J. R.; Gray, H. B. *Science* **1992**, *256*, 1007. (g) Wuttke, D. S.; Bjerrum, M. J.; Chang, I.-J.; Winkler, J. R.; Gray, H. B. *Biochim. Biophys. Acta* **1992**, *1101*, 168.

(17) Winkler, J. R.; Gray, H. B. *Chem. Rev.* **1992**, *92*, 369.

(18) Moser, C. C.; Keske, J. M.; Warncke, K.; Farid, R. S.; Dutton, P. L. *Nature* **1992**, *355*, 796.

(19) Axup, A. W.; Albin, M.; Mayo, S. L.; Crutchley, R. J.; Gray, H. B. *J. Am. Chem. Soc.* **1988**, *110*, 435.

(20) (a) Oevering, H.; Paddon-Row, M. N.; Heppener, M.; Oliver, A. M.; Cotsaris, E.; Verhoeven, J. W.; Hush, N. S. *J. Am. Chem. Soc.* **1987**, *109*, 3258. (b) Paddon-Row, M. N.; Oliver, A. M.; Warman, J. M.; Smit, K. J.; DeHaas, M. P.; Oevering, H.; Verhoeven, J. W. *J. Phys. Chem.* **1988**, *92*, 6952. (c) Oevering, H.; Verhoeven, J. W.; Paddon-Row, M. N.; Warman, J. M. *Tetrahedron* **1989**, *45*, 4751. (d) Warman, J. M.; Hom, M.; Paddon-Row, M. N.; Oliver, A. M.; Kroon, J. *Chem. Phys. Lett.* **1990**, *172*, 114. (e) Kroon, J.; Verhoeven, J. W.; Paddon-Row, M. N.; Oliver, A. M. *Angew. Chem.* **1991**, *30*, 1358.

(21) Closs, G. L.; Miller, J. R. *Science* **1988**, *240*, 440.

(22) (a) Isied, S. S.; Vassilian, A.; Wishart, J. F.; Creutz, C.; Schwarz, H.; Sutin, N. *J. Am. Chem. Soc.* **1988**, *110*, 635. (b) Vassilian, A.; Wishart, J. F.; van Hemelryck, B.; Schwarz, H.; Isied, S. S. *J. Am. Chem. Soc.* **1990**, *112*, 7278.

(23) Miller, J. R.; Beitz, J. V.; Huddleston, R. K. *J. Am. Chem. Soc.* **1984**, *106*, 5057.

(24) Strauch, S.; McLendon, G.; McGuire, M.; Guarr, T. *J. Phys. Chem.* **1983**, *87*, 3579.

(25) (a) Domingue, R. P.; Fayer, M. D. *J. Chem. Phys.* **1985**, *83*, 2242. (b) Dorfman, R. C.; Lin, Y.; Zimmt, M. B.; Baumann, J.; Domingue, R. P.; Fayer, M. D. *J. Phys. Chem.* **1988**, *92*, 4258.

(26) Gust, D.; Moore, T. A. *Science* **1989**, *244*, 35.

0002-7863/93/1515-1485$04.00/0

Deviations from an exponential distance dependence are expected if the specific composition of the intervening polypeptide is important in determining the coupling. This circumstance has been addressed theoretically by Beratan and Onuchic by using an electronic-coupling pathway model.[6,7] In this model the coupling between donor and acceptor in a protein is described in terms of physical tunneling pathways comprised of covalent, H-bonded, and through-space contacts. Using a searching algorithm and the protein crystal structure coordinates, optimum coupling pathways can be identified.[7c] The optimum pathway can be described in terms of an effective covalent pathway and then in terms of a σ-tunneling length (σl, 1.4 Å times the nonintegral number of covalent bonds in the effective path). The pathway model predicts that ln k_{max} will vary linearly with σl with slope β'. The current parameterization of the model uses a coupling-decay factor of 0.6 for each covalent bond[6,7] that defines $\beta' = 0.73$ Å^{-1} and implies that the intramolecular ET rate drops by 2 orders of magnitude for every 6.3-Å increase in the σ-tunneling length. This approach has been used successfully to describe the coupling in Ru-modified cytochromes *c*, systems in which the homogeneous barrier model fails to predict the experimentally determined couplings.[16f,g]

Within the confines of the pathway model, Beratan, Betts, and Onuchic have examined the effects of protein secondary and tertiary structure on distant electronic couplings.[6] In contrast to the predictions of Dutton's homogenous barrier analysis,[18] they estimate that average values of β can vary from 1.0 to 1.5 Å^{-1} for different proteins.[6] For myoglobin (Mb) (79% α-helix) and cytochrome *c* (51% α-helix), the average β values are 1.4 and 1.2 Å^{-1}, respectively, suggesting similar decays with distance for these two proteins.[6] The pathway model suggests one important distinction between Mb and cytochrome *c*: many equivalent pathways are found in Mb, while a small number of paths tend to dominate the coupling in cytochrome *c*. This difference may be a reflection of differing degrees of inhomogeneity in the polypeptides of the two proteins.

These theoretical considerations have prompted us to examine the ET kinetics in three Ru-modified human myoglobin (HuMb) mutants in order to provide a direct comparison to our data[16f-h] on Ru-modified cytochromes *c*. HuMb mutants were selected to provide donor–acceptor distances in the same range (10–15 Å) as that examined in cytochrome *c*. The following mutant proteins, each containing a single surface-modifiable histidine at a fixed distance, have been prepared: His70, $d = 9.5$ Å; His48, 12.7 Å; and His83, 15.5 Å (Figure 1). Each mutant protein has been derivatized by coordination of a pentaammineruthenium (a_5Ru) complex to the surface His.[17] Rates of intramolecular $^3ZnP^* \rightarrow Ru^{3+}$ and $Ru^{2+} \rightarrow ZnP^+$ (P = mesoporphyrin IX diacid) reactions have been measured using transient absorption spectroscopy.

Experimental Section

Materials and Equipment. All DNA-modifying enzymes were purchased from New England Biolabs and Boehringer Mannheim Biochemicals. Oligonucleotides necessary for the mutagenesis were obtained from the Applied Microchemical Facility at Caltech and were purified by dialysis or gel filtration. The *Escherichia coli* strain CJ236 (*dut, ung, thi, relA,* pCJ105(*Cm'*)) and the strain MV1190 (Δ(*lac-proAB*), *thi, supE,* Δ(*srl-recA*)306::Tn10(*tet'*)F':*traD36, proAB, lac I^{q}ZΔ*M15*) were obtained from Bio-Rad. All chromatographic products such as DEAE-Sepharose resin and Mono-S HR cation-exchange columns were purchased from Pharmacia. Electronic absorption spectra were measured on a Hewlett-Packard Model 8452A diode array spectrophotometer.

Distilled water circulated through a Barnstead Nanopure water purification system (specific resistance > 18 MΩ·cm) was used in the preparation of all aqueous solutions. Sodium phosphate (NaP_i) and 4-(2-hydroxyethyl)-1-piperazineethanesulfonic acid (HEPES) buffers were prepared with analytical grade reagents. 2-Butanone (MCB) was stored over aluminum oxide (Woelm neutral, Waters Associates) at 4 °C to prevent the accumulation of peroxides. Aquopentaammineruthenium(II) ($a_5Ru(OH_2)^{2+}$) was synthesized by reduction of chloropentaammineruthenium(III) (Strem) by zinc amalgam.[27] The $a_5Ru(OH_2)^{2+}$ solution was used directly in the labeling reaction with protein. The preparation of zinc mesoporphyrin IX diacid (ZnP) has been described.[19] All other reagents and solvents were of the highest grade available and were used without further purification. Concentration of protein solutions, removal of small molecules, and buffer exchanges were performed on an Amicon ultrafiltration system (YM-10 membranes, 10-kDa molecular weight cutoff) or a Centricon-10 ultraconcentrator (Amicon).

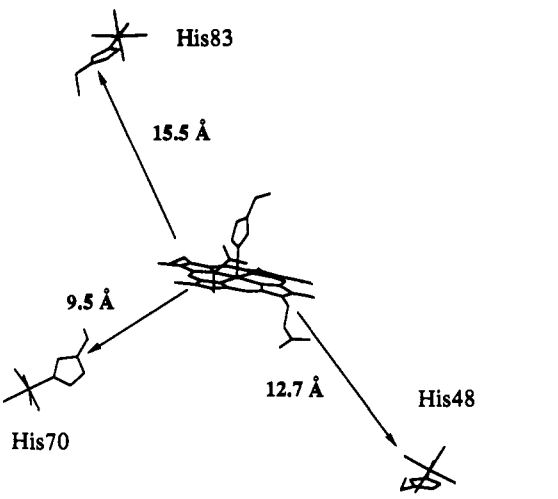

Figure 1. Computer-generated model of the structures of the redox sites in a_5Ru(His*X*)/ZnP-HuMb (*X* = 48, 70, 83) derivatives based on the 1.6-Å crystal structure[35] of the wild-type protein.

Site-Directed Mutagenesis and Protein Isolation. HuMb contains a single buried cysteine (position 110) that sometimes complicates the purification of genetically engineered apoproteins.[28] All of our proteins incorporate the Cys110Ala mutation to eliminate the possibility of dimer formation during purification. The gene for human Mb containing a Cys → Ala mutation at position 110 and a suitable expression system in *E. coli* were provided by S. G. Boxer of Stanford University. Standard protocols for DNA manipulations and cell transformations were performed as described by Sambrook.[29] HuMb contains two surface accessible histidines (His48 and His81). Construction of the C110A/H48Q (i.e., containing only the codon for His81) and the C110A/H81Q (i.e., containing only the codon for His48) HuMb genes and subsequent protein expression were performed as described previously.[30]

Prior to the introduction of surface histidines other than the naturally occurring residues, a hybrid M13mp19FX-H48Q/H81Q/C110AHuMb plasmid was constructed via a three-fragment ligation. A 243-bp *Bam*HI-*Afl*II restriction fragment of the pMbQ48 (pLcIIFX shuttle vector containing the H48Q/C110A HuMb gene) and a 505-bp *Afl*II-*Hin*dIII restriction fragment of pMbQ81 (pLcIIFX shuttle vector containing the H81Q/C110A HuMb gene) were cloned into the polylinker site of M13mp19RF by mixing in a 5:5:1 ratio and adding T4 DNA ligase. All oligonucleotide-directed mutagenesis was performed on the single-stranded form of this hybrid plasmid following a standard method.[31] The primers for oligonucleotide-directed mutagenesis of codons 70 (ACC thr to CAT his) and 83 (GAG glu to CAT his) were 5'-ACT-GTG-CTC-CAT-GCC-CTG-GGT-3' for the T70H mutant and 5'-GGG-CAA-CAT-CAT-GCA-GAG-ATT-A-3' for the E83H mutant. Full gene sequences were obtained by the dideoxy method.[32] The 0.75-kb *Bam*HI-*Hin*dIII fragment containing the mutant HuMb genes was subcloned

(27) Ford, P.; Rudd, De F. P.; Gaunder, R.; Taube, H. *J. Am. Chem. Soc.* **1968**, *90*, 1187.

(28) (a) Varadarajan, R.; Szabo, A.; Boxer, S. G. *Proc. Natl. Acad. Sci. U.S.A.* **1985**, *82*, 5681. (b) Varadarajan, R.; Lambright, D. G.; Boxer, S. G. *Biochemistry* **1989**, *28*, 3771. (c) Hubbard, S. R.; Hendrickson, W. A.; Lambright, D. G.; Boxer, S. G. *J. Mol. Biol.* **1990**, *213*, 215.

(29) Sambrook, J.; Fritsh, E. F.; Maniatis, T. *Molecular Cloning: A Laboratory Manual*; Cold Spring Harbor Laboratory: Cold Spring Harbor, NY, 1989.

(30) Zewert, T. E. Ph.D. Thesis, California Institute of Technology, Pasadena, CA, 1990.

(31) Kunkel, T. A. *Proc. Natl. Acad. Sci. U.S.A.* **1985**, *82*, 488. The Muta-Gene oligo-directed mutagenesis kit from Bio-Rad was used to carry out this procedure.

(32) Sanger, F.; Nicklen, S.; Coulson, A. R. *Proc. Natl. Acad. Sci. U.S.A.* **1977**, *74*, 5463. The Sequenase version 2.0 kit from United States Biochemicals was used to carry out this procedure. The kit supplies a genetically altered T7 DNA polymerase (Sequenase) instead of *E. coli* DNA poll to perform primer extension.

into the pLcII vector to yield the corresponding pMb plasmids. The expression vector was introduced into *E. coli* strain AR68 (*lac*^{amber}, *trp*^{amber}, *pho*^{amber}, *sub*^{cts}, *Str*^{r}, *hdpr*, *galE*::Tn110(λ*c*I857, Δ*Bam*, Δ*HI*, *bio*, *uvrB*) *Tet*^{r}) by electroporation (0.2-cm cuvettes, 2.5-kV applied voltage, 25 μF, 200 Ω) using a Bio-Rad Gene Pulser apparatus. The cell cultures were grown at the 170-L fermentation facility of the UCLA Molecular Biology Institute. Conditions for cell growth, temperature induction, apoprotein isolation, and heme reconstitution followed those outlined by Varadarajan et al.[28]

Surface Modification and Heme Replacement. Covalent modification of the HuMb surface histidine with pentaammineruthenium (a_5Ru) and subsequent replacement of the heme with ZnP were performed as described previously (with minor modifications).[19] The proteins were reacted with a 25-fold excess of freshly generated $a_5Ru(OH_2)^{2+}$ under argon for 4–6 h. The reaction was quenched by gel filtration and oxidation with Co(phenanthroline)$_3^{3+}$. The reaction products were then separated on a Mono S (HR 10/10 or 10/16, Pharmacia) cation-exchange column fitted to a Pharmacia FPLC system. The samples were loaded in 50 mM NaP_i buffer, pH 5.5, and eluted with a linear gradient of 50 mM NaP_i, 1.0 M NaCl, pH 6.5. The heme of the ruthenium-modified protein was extracted by HCl/butanone treatment; reconstitution with zinc mesoporphyrin IX diacid followed established procedures.[19,33] The ZnP-reconstituted proteins were purified using the same chromatographic conditions described above. Sample purity was confirmed by a A_{414}/A_{280} ratio of ca. 16 ($\epsilon_{414} \sim 250$ mM^{-1} cm^{-1}). All manipulations of the ZnP-reconstituted proteins were performed with the exclusion of room light.

Kinetics Measurements. Fully oxidized protein samples (0.5–10 μM protein concentration in μ = 100 mM NaP_i, pH 7.0) were transferred into vacuum cells having 1-cm cuvette side arms.[34] The samples were degassed and purged with purified argon on a dual-manifold vacuum argon line incorporating a manganese oxide scrubbing column to remove residual oxygen. At least 10 vacuum/fill cycles were used to deoxygenate samples, taking care not to denature the protein by bubbling. The deoxygenated samples were excited with pulses from the second harmonic of a Q-switched Nd:YAG laser (532 nm, 10-ns fwhm). ZnP triplet-state (^{3}ZnP*) decay kinetics were monitored by transient absorption measurements at 450 nm. Charge–recombination kinetics were measured by following the ZnP radical cation (ZnP^+) at 380 nm.

Molecular Modeling. All computer graphics and related calculations were performed using BIOGRAF version 2.1 (BioDesign, Inc.) on a VaxStation 3500. Results were displayed on an Evans and Sutherland PS390 terminal. The refined coordinates for HuMb were obtained from a 1.6-Å resolution X-ray structure of a C110A/K45R mutant.[35] Minimized structures of the modified histidines were obtained after searching the conformational spaces generated by rotating the C_α–C_β and C_β–C_γ bonds. Only those van der Waals and electrostatic interactions within 9 Å of the ruthenium-labeled histidine were included in the calculations. Intramolecular distances were deduced from the minimized structures.[36]

Pathway Searches. Tunneling pathways in Ru-modified proteins were identified using software written in FORTRAN for Silicon Graphics IRIS and INDIGO computers. This software is based on a search algorithm developed by Beratan, Betts, and Onuchic.[7g] The pathway searches determine relative coupling strengths for pathways connecting two sites in a protein.

Results and Discussion

Mutagenesis, Modification, and Characterization. In order to simplify preparation and purification of the singly Ru-modified proteins, site-directed mutants of HuMb having only one surface histidine were constructed. In the case of His48 HuMb, His81 was changed to glutamine. For His70 HuMb and His83 HuMb, both His48 and His81 were replaced with glutamines. The gene products were primarily expressed as 21-kDa fusion proteins.

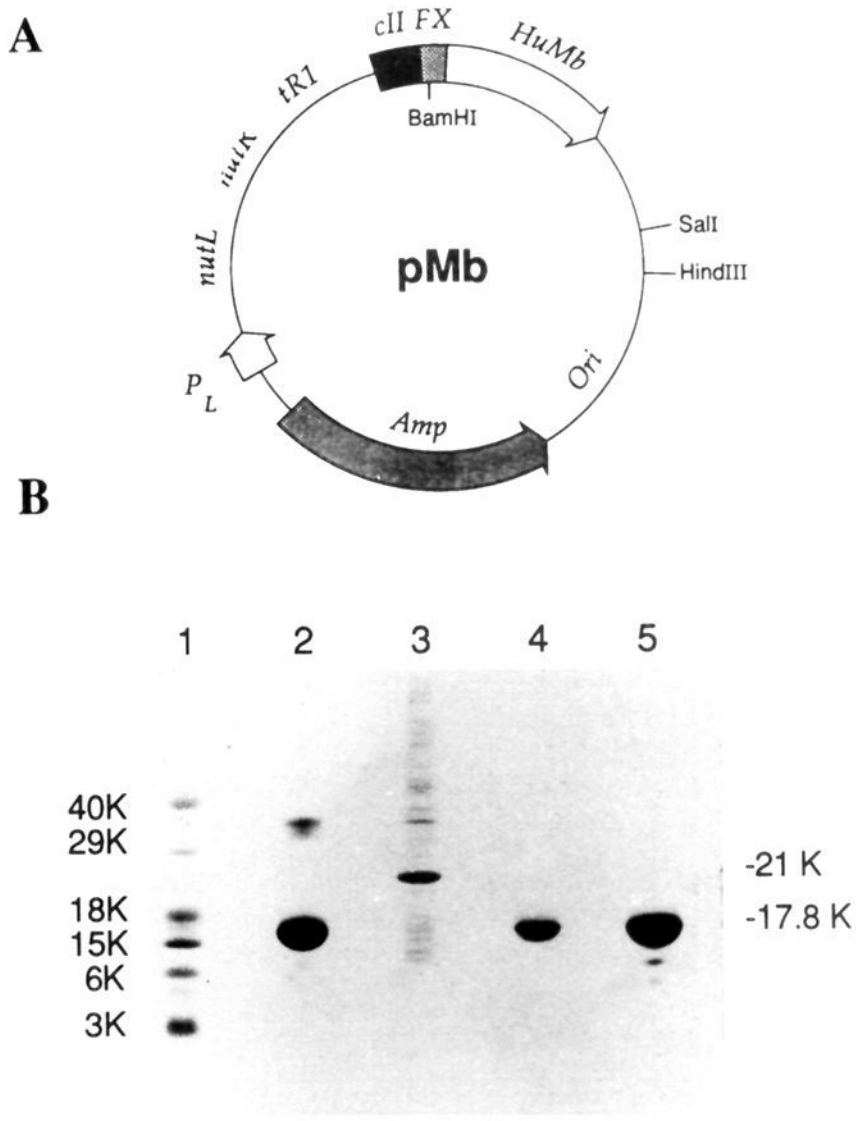

Figure 2. (A) Construction of pMb. By raising the growth temperature to 42 °C, the plasmid directs the production of a 21-kDa fusion protein consisting of 31 amino-terminal residues of λ *c*II protein, the factor X_a cleavage site (F*X*), and HuMb.[28] (B) PAGE-SDS gel of HuMb gene products. Lane 1, MW standards; lane 2, sperm whale Mb (Sigma); lane 3, total cellular proteins of *E. coli* harboring pMb-(His70) HuMb after temperature induction; lane 4, mature His70 HuMb protein after heme reconstitution and tryptic digestion; and lane 5, mature His83 HuMb holoprotein.

Subsequent heme reconstitution and limited tryptic digestion yielded mature holoproteins having the correct molecular weight (Figure 2).[30] The mutants exhibit the same UV/vis spectral properties (in all oxidation states) as the wild-type proteins.

For each of the mutant proteins, the reaction with the pentaammineruthenium complex was highly specific (monitored by ion-exchange chromatography). The retention volumes of the unmodified and modified proteins correlate with the overall positive charge on the protein surface. In each chromatogram, the unmodified protein elutes first, followed by the singly modified protein. The a_5Ru(His70) HuMb derivative elutes earlier in the gradient than the a_5Ru(His83) mutant; His70 HuMb incorporates a threonine-to-histidine mutation, whereas His83 HuMb involves loss of a surface glutamic acid residue.

ET Kinetics. ET in the a_5Ru/ZnP-substituted HuMbs was initiated by pulsed-laser excitation of ZnP. The ^{3}ZnP* excited state is long-lived (20 ms) and highly reducing ($E° \sim -0.74$ eV vs NHE).[19] In addition to its usual deactivation processes, ^{3}ZnP* can decay by electron transfer to a surface Ru^{3+}. The subsequent electron-hole recombination reaction ($Ru^{2+} \rightarrow ZnP^+$ ET) regenerates the original species. The reactions were monitored at wavelengths where the transient absorption arises mainly from ^{3}ZnP* (450 nm) or ZnP^+ (380 nm).

The triplet decay for a_5Ru(His70)/ZnP-HuMb monitored at 450 nm is, in principle, the sum of the intrinsic decay rate (k_d = 50 s^{-1}) and the ^{3}ZnP* → Ru^{3+} rate (k_f(ET)). A fit to a single exponential expression gives a rate constant of 1.6×10^7 s^{-1} that is independent of protein concentration between 0.5 and 10 μM. This 10^5-fold increase in the triplet decay rate compared to unmodified Mb indicates that the ET channel is an efficient decay pathway. The charge-recombination signal was too fast to be

(33) (a) Teale, F. W. J. *Biochim. Biophys. Acta* **1959**, *35*, 543. (b) Yonetani, T. *J. Biol. Chem.* **1967**, *242*, 5008. (c) Cowan, J. A.; Gray, H. B. *Inorg. Chem.* **1989**, *28*, 2074.

(34) Marshall, J. L.; Hopkins, M. D.; Gray, H. B. *ACS Symp. Ser.* **1987**, *357*, 254.

(35) Hubbard, S. R.; Hendrickson, W. A.; Lambright, D. G.; Boxer, S. G., unpublished results.

(36) A rigid-geometry search of Ru-modified histidine conformations was performed by successively rotating the two side-chain dihedral angles by 18° from 0 to 360° (Shih, H. H.-L.; Brady, J.; Karplus, M. *Proc. Natl. Acad. Sci. U.S.A.* **1985**, *82*, 1695). The most stable 20 conformers were examined for any unfavorable van der Waals ($d < 3$ Å) contacts. Because interconversions among different conformers are expected to be extremely rapid (Brooks, C. L., III; Karplus, M.; Pettitt, B. M. *Adv. Chem. Phys.* **1988**, *71*, 95), the shortest donor–acceptor distances are given for the modified proteins.

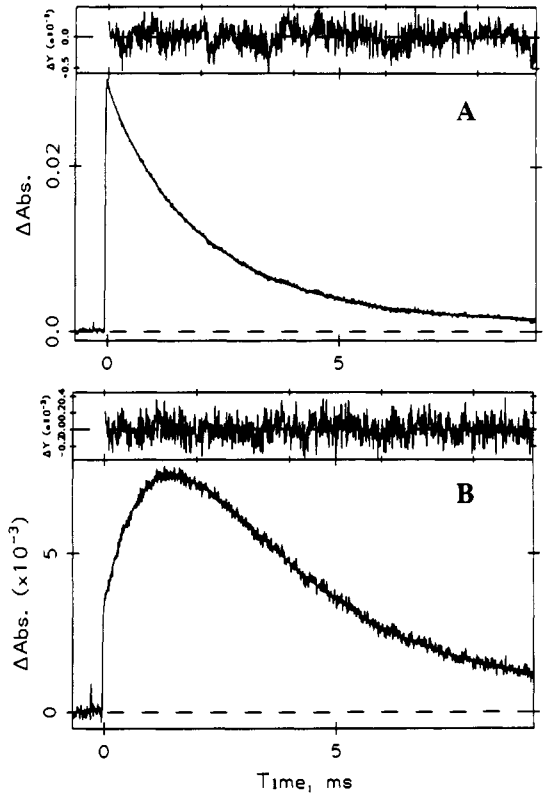

Figure 3. Transient kinetics of a_5Ru(His83)/ZnP-HuMb (532-nm excitation; 10-ns pulse width; 2-μM sample concentration). (A) Absorbance changes monitored at 450 nm; the smooth line is a fit to an exponential decay function with $k_{obsd} = 4.5 \times 10^2$ s^{-1}. (B) Absorbance changes monitored at 380 nm; the smooth line is a fit to a biexponential decay function with rate constants 4.5×10^2 and 7.3×10^2 s^{-1}.

resolved from the instrument response.

Figure 3 illustrates the triplet decay and charge-recombination signals for the a_5Ru(His83)/ZnP derivative. Similar data were obtained for a_5Ru(His48)/ZnP-HuMb. Transient absorption signals at 380 nm were fit to biexponential decay functions in which the rise of the signal corresponds to the charge–recombination process and the decay component matches the observed triplet decay rates (measured at 450 nm). The insensitivity of the observed rates to changes in protein concentrations ranging from 0.5 to 10 μM rules out the possibility of bimolecular contributions to the observed rates. The charge-recombination rates (His48, $k_{cr} = 1.1 \times 10^5$; His83, 7.3×10^2 s^{-1}) are inherently faster than the forward rates (His48, k_f(ET) = 7.2×10^4; His83, 4.0×10^2 s^{-1}), owing to the higher driving force for the back reaction ($-\Delta G° = 0.96$ eV as compared to 0.82 eV for the forward reaction).[17] It is interesting to note that the forward rate for the His48 HuMb derivative is essentially identical with that observed previously for the equivalent His48 sperm whale Mb derivative (k_f(ET) = 7.0×10^4 s^{-1});[19,37] this result was not unexpected, because the structures of these two proteins are closely similar.[28,35]

Distant Electronic Couplings. In order to compare electronic couplings in the Ru-modified proteins, the nuclear terms must be factored from the observed ET rates.[2] The driving force for the ^{3}ZnP* → Ru^{3+} ET is 0.82 eV.[17,19,38] A study of the driving-force dependence of ET rates in metal-substituted Ru(His48)Mb indicates that the reorganization energy λ is ~1.3 eV.[17] Assuming a similar value of λ for Ru(His70)Mb and Ru(His83)Mb, values of k_{max} can be extracted using the semiclassical Marcus expression[2] for nonadiabatic ET rates: 7.2×10^7 s^{-1} (His70, d = 9.5); 3.3×10^5 s^{-1} (His48, d = 12.7); and 1.8×10^3 s^{-1} (His83, d = 15.5 Å).

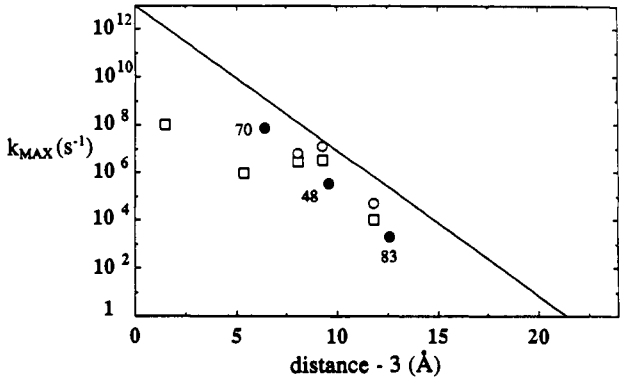

Figure 4. Variation of k_{max} with distance d for a_5Ru/ZnP derivatives of HuMb (●) and cytochrome c (○),[16c] and Ru(bpy)$_2$(im)(His)-cytochrome c (□).[16f,g] The solid line is based on eq 1 with $\beta = 1.4$ Å^{-1} and a maximum ET rate of 10^{13} s^{-1} at close contact. The plot was constructed using edge-edge distances between redox sites.

Table I. ET Parameters for HuMb and Cytochrome c Derivatives

mutant	no. of paths[a]	edge–edge σ1, Å: dominant path	edge–edge σ1, Å: multiple paths	k_{max}, s^{-1} [b]
His70Mb	106	24.3	15.7	7.2×10^7
His48Mb	79	37.5	29.9	3.3×10^5
His83Mb	186	43.5	32.5	1.8×10^3
His79cyt	3	11.2	10.3	($\geq 10^8$)
His39cyt	1	19.7	19.7	1.4×10^7 (3.3×10^6)
His33cyt	5	19.4	16.1	2.9×10^6 (2.7×10^6)
His72cyt	11	24.7	20.2	(9.4×10^5)
His62cyt	22	28.9	22.5	2.0×10^4 (1.0×10^4)

[a] Number of pathways with H_{AB} within an order of magnitude of the best pathway. [b] Values of k_{max} correspond to ^{3}ZnP* → Ru^{3+} ET, whereas the activationless rates in parentheses refer to Fe^{2+} → Ru^{3+} ET in Ru(bpy)$_2$(im)(His)-modified proteins (refs 16f,g).

A plot of log k_{max} vs d for the three a_5Ru(His)/ZnP derivatives of HuMb is shown in Figure 4, along with data for previously characterized a_5Ru/ZnP- and Ru(bpy)$_2$(im)(His)-modified cytochromes c (bpy = 2,2′-bipyridine; im = imidazole). The solid line is that proposed by Dutton and co-workers for ET in proteins ($\beta = 1.4$ Å^{-1}).[18] The k_{max} values for all of the Ru-modified proteins fall below the line and are not well-correlated with d. Indeed, a strong argument against the homogeneous barrier model arises from the observation that Ru derivatives of Mb and cytochrome c having similar values of d exhibit quite different values of k_{max}. The scatter of the data points in this plot reflects the inhomogeneous nature of the media between redox sites. It is possible, nevertheless, to define an average β for these data; values of 1.4 and 1.2 Å^{-1} have been proposed for Mb and cytochrome c.[13] It is apparent from Figure 4 that most of the data points would be in the vicinity of a $\beta \sim 1.4$ Å^{-1} line that had a somewhat lower intercept. The difference between such a correlation and Dutton's $\beta = 1.4$ Å^{-1} line[18] may be the result of inconsistent or uncertain distance measurements. Analysis of the rate data using metal-to-porphyrin edge (ZnP systems) and metal-to-metal (Ru(bpy)$_2$(im)(His) systems) distances instead of edge–edge distances reduces somewhat the systematic deviations but does not eliminate the scatter.

It is clear that we must consider inhomogeneous models in order to gain a deeper understanding of the factors controlling electronic couplings in Ru-modified proteins. In prior work, we have analyzed Ru-modified cytochrome c ET rates in terms of the Beratan–Onuchic pathway model.[6,7,16f,g] This approach explicitly accounts for the inhomogeneities of the medium separating donor

(37) ET rates for the three sperm whale myoglobin derivatives with the longest D–A separations (His12, His116, His81) are not included in this analysis because unresolved bimolecular contributions to the observed rates make the reported values at best upper limits to the true intramolecular ET rates.[17]

(38) (a) Crutchley, R. J.; Ellis, W. R.; Gray, H. B. *J. Am. Chem. Soc.* **1985**, *107*, 5002. (b) Karas, J. L.; Lieber, C. M.; Gray, H. B. *J. Am. Chem. Soc.* **1988**, *110*, 599. (c) Karas, J. L. Ph.D. Thesis, California Institute of Technology, Pasadena, CA, 1989.

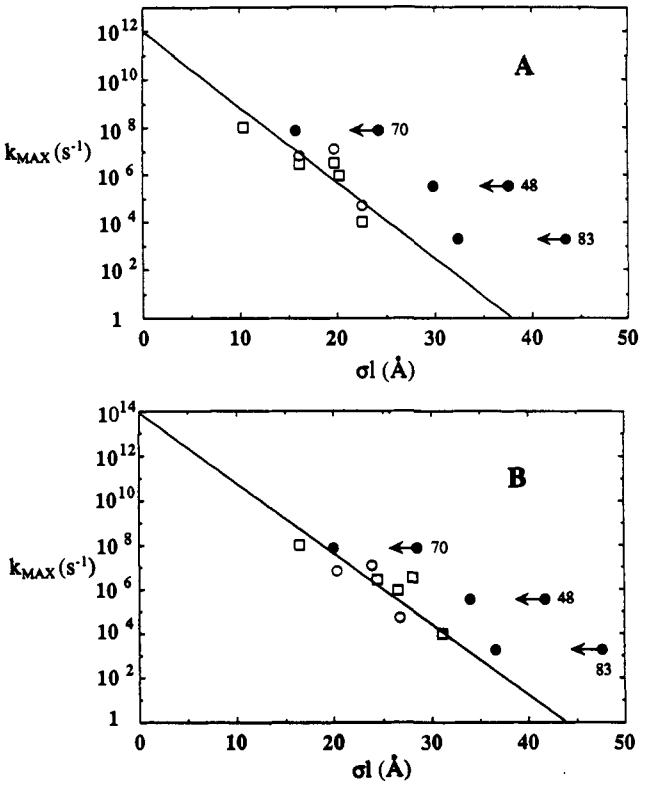

Figure 5. Variation of k_{max} with multiple-pathway tunneling lengths (σl) for a_5Ru/ZnP derivatives of HuMb (●) and cytochrome *c* (○),[16c] and Ru(bpy)$_2$(im)(His)-cytochrome *c* (□).[16f-h] Correlations with edge–edge (A) and Ru–edge (B) σ-tunneling lengths. Points with left arrows indicate the dominant path tunneling lengths for a_5Ru/ZnP-HuMb.

and acceptor. In the simplest formulation of the pathway model, a single route is assumed to dominate the D–A coupling.[7] This assumption seems to be justified for cytochrome *c*, where k_{max} correlates well with σl for the dominant paths. With Ru-modified Mb, however, the rates are not in accord with σl values (Figure 5). Furthermore, the Mb points are all systematically offset from the cytochrome *c* points. The pathway searches reveal a significant distinction between Mb and cytochrome *c*: a small number of paths dominates the coupling in cytochrome *c*, while a great many more nearly equivalent paths can be found in Mb. Table I lists the number of paths with couplings within a factor of 10 of the best path for each of the Ru-modified proteins that we have studied.[39] Fewer than 20 paths contribute in cytochrome *c*, while nearly 10 times that number are found in some Mb derivatives. If just the best route is used to calculate σl in Mb, then several near-optimum routes will be neglected. Many tunneling pathways contributing to the D–A coupling should substantially increase the overall coupling. If a sufficiently large number of paths contributes to the total electronic coupling, then the explicit nature of one path becomes unimportant and tunneling lengths should closely parallel edge–edge distances.

The large number of pathways obtained for HuMb compared to cytochrome *c* clearly demonstrates that in some systems the dominant pathway model must be modified to account for the contributions from nearly equivalent pathways.[7e] Accordingly, we have calculated overall couplings as the sum of the couplings for the individual pathways in both Mb and cytochrome *c* (Table I). The multiple-pathway couplings were converted to edge–edge σ-tunneling lengths as was done for single pathways. The results of this analysis appear in Figure 5a. The solid line has the required distance decay of 0.73 Å^{-1}. The cytochrome *c* data still correlate reasonably well with σl, and the offset of the Mb data has been reduced. It is important to note that electron transfers involving native Fe-cytochrome *c* and Zn-substituted cytochrome *c* correlate well with the same $\beta' = 0.73$ Å^{-1} line. The deviations of the Mb data, then, are not likely the result of differences in ZnP and FeP ET reactions.

A successful correlation of k_{max} values with distance (either *d* or σl) requires that rates extrapolate to a single close-contact value. A consistent measure of D–A distance is, therefore, essential. Part of the poor correlation of the Ru-modified Mb data with σl could be due to the edge-to-edge distance scale, because this scale implicitly assumes that the coupling involves donor and acceptor orbitals that are delocalized over the ligands. It has been shown that H_{AB} for two contacting metal complexes depends upon the square of the metal–ligand orbital mixing coefficient.[40] If the metal–ligand mixings in Ru-modified HuMb are relatively small, then the σ tunnels should extend to the Ru-atom redox centers rather than stopping at the ligands. The donor wave function of ^{3}ZnP*, however, is delocalized over the porphyrin, and it is reasonable to measure pathways to the porphyrin edge in ZnP electron transfers. Figure 5b presents a plot of log k_{max} values versus the Ru-to-porphyrin edge tunneling lengths, i.e., adding σ bonds of the ligands and the metal–ligand bonds to the edge-to-edge paths. Also shown are the corresponding data for Ru(bpy)$_2$(im)(His)- and a_5Ru/ZnP-cytochrome *c*. A slightly improved fit of the cytochrome *c* data is found; the best constrained β' fit of log k_{max} vs Ru-to-edge σl for the cytochrome *c* data shows a marked difference in the calculated one-bond-limit ET rates: 10^{14} s^{-1} for the Ru–edge or Ru–Fe scale and 10^{12} s^{-1} for the edge-to-edge scale.

The failure of a single-pathway model to describe adequately the electronic couplings in Mb may be a characteristic of non-ET proteins; specific ET routes between redox sites offer no functional advantage. Although inclusion of multiple tunneling pathways does move the Ru-modified Mb data points in the right direction, the correlation of k_{max} with σl is not completely satisfactory. Our analysis assumes only constructive interference among pathways; more sophisticated treatments of distant electronic couplings in model complexes and proteins, however, identify an important role for destructively interfering multiple pathways.[7e,9b,40] A particular characteristic of Mb, the flexibility of the porphyrin in the heme pocket,[41] also may be a complicating factor. Pathway analyses are based on crystal structure coordinates, but the dynamics of porphyrin motion could influence ET rates in Mb. The tunneling pathway model is a first attempt to describe D–A coupling across inhomogeneous media and may simply lack the complexity necessary to describe the couplings in Mb. More sophisticated treatments of D–A couplings in Ru-modified cytochromes *c* (which are well-described by the tunneling pathway model) have yielded remarkable agreement between experimental and calculated values of H_{AB}.[8b,9b] It is possible that similar analyses will be able to account for the distant electronic couplings in Mb.

Acknowledgment. We thank David N. Beratan for helpful discussions, Atsuo Kuki for a preprint of ref 9b, Steven G. Boxer for the HuMb gene, and David G. Lambright, Steve R. Hubbard, and Wayne A. Hendrickson for providing us with the coordinates of a mutant human myoglobin. We are indebted to Thomas Sutherland for performing the large cell growth. J.L.C. acknowledges support from an NSF postdoctoral fellowship (CHE-9002195) and L.-L.W. thanks SERC (United Kingdom) for a NATO postdoctoral fellowship. This research was supported by the National Science Foundation, the National Institutes of Health, and the Arnold and Mabel Beckman Foundation.

(39) The pathway searches were conducted with two user-defined parameters that affect the number of pathways identified.[7e] One parameter was set to require that a through-space jump between two atoms having a decay constant $\epsilon_s \geq 0.90$ times that of an alternative through-bond route be included in the connectivity list. The second parameter requires that pathways with H_{AB} greater than or equal to 50% of the current best pathway H_{AB} will be saved.

(40) Newton, M. D. *J. Phys. Chem.* **1988**, *92*, 3049.
(41) (a) Karplus, M.; McCammon, A. D. *CRC Crit. Rev. Biochem.* **1981**, *9*, 293. (b) La Mar, G. N.; Haukson, J. B.; Dugad, L. B.; Lidell, P. A.; Venkataramana, N.; Smith, K. M. *J. Am. Chem. Soc.* **1991**, *113*, 1544.